To cite this version :

Maxim VAN DEN ABBEELE, Jean-Marc VALIADIS, Lucas Venancio LIMA, Pascal KHALIFE, Wafa SKALLI, Philippe ROUCH - Contribution to FE modeling for intraoperative pedicle screw strength prediction - Computer Methods in Biomechanics and Biomedical Engineering - Vol. 21, n°1, p.13-21 - 2017

Contribution to FE modeling for intraoperative pedicle screw strength prediction

Maxim Van den Abbeele, Jean-Marc Valiadis, Lucas V. P. C. Lima, Pascal Khalifé, Philippe Rouch and Wafa Skalli

Institut de Biomécanique Humaine Georges Charpak, Arts et Métiers ParisTech, 151, Boulevard de l'Hopital, Paris, 75013, France

ABSTRACT

Although the use of pedicle screws is considered safe, mechanical issues still often occur. Commonly reported issues are screw loosening, screw bending and screw fracture. The aim of this study was to develop a Finite Element (FE) model for the study of pedicle screw biomechanics and for the prediction of the intraoperative pullout strength. The model includes both a parameterized screw model and a patient-specific vertebra model. Pullout experiments were performed on 30 human cadaveric vertebrae from ten donors. The experimental force-displacement data served to evaluate the FE model performance. μCT images were taken before and after screw insertion, allowing the creation of an accurate 3D-model and a precise representation of the mechanical properties of the bone. The experimental results revealed a significant positive correlation between bone mineral density (BMD) and pullout strength (Spearman $\rho = 0.59$, $p < 0.001$) as well as between BMD and pullout stiffness (Spearman $\rho = 0.59$, $p < 0.001$). A high positive correlation was also found between the pullout strength and stiffness (Spearman $\rho = 0.84$, $p < 0.0001$). The FE model was able to reproduce the linear part of the experimental force-displacement curve. Moreover, a high positive correlation was found between numerical and experimental pullout stiffness (Pearson $\rho = 0.96$, $p < 0.005$) and strength (Pearson $\rho = 0.90$, $p < 0.05$). Once fully validated, this model opens the way for a detailed study of pedicle screw biomechanics and for future adjustments of the screw design.

1. Introduction

In the United States alone, the number of spinal fusion surgeries increased by 240%, from approximately 174,000 to 413,000 surgeries, between 1998 and 2008 (Rajaee et al. 2012). In 2005, nearly 150,000 similar interventions were performed in Germany, France, Italy, Spain and the UK (MedTech Insight 2006). Although the use of pedicle screws is widespread and considered safe (Faraj and Webb 1997; Lonstein et al. 1999), mechanical complications remain prevalent. Commonly reported issues are screw bending, breakage and loosening (Faraj and Webb 1997; Lonstein et al. 1999; Hsu et al. 2005; Chatzistergos et al. 2010; Chamoli et al. 2014; Prud'homme et al. 2014). In non-fusion techniques, in which the implant stays functional during the patient's lifetime, screw loosening and breakage may lead to loss of function (Prud'homme et al. 2014). In spinal fusion, where temporary stabilization (6 to 9 months) is sufficient, these complications may yield pseudarthrosis or incomplete fusion (Hadjipavlou et al. 1996; Lonstein et al. 1999). For patients with decreased bone quality, spinal stabilization is even more complex due to a drastically reduced screw pullout strength (Okuyama et al. 2001). A thorough understanding of the mechanical screw-bone interaction is necessary when facing these issues.

Literature describes the use of *in vitro* tests, such as pullout, fatigue, bending and insertional torque tests, to evaluate the performance of pedicle screws inserted in bone-mimicking polyurethane (PU) foam (Hsu et al. 2005; Chao et al. 2008; Kim et al. 2012; Arslan et al. 2013; Amaritsakul et al. 2014; Cetin et al. 2015; Demir and Basgül 2015) or in animal vertebrae (Demir et al. 2012; Demir and Basgül 2015; Yaman et al. 2015; Aycan et al. 2017) and of bone screws (Shirazi-Adl et al. 1994), for which however the loading conditions and the screw/bone interactions are different. In most cases, the specifications of the American Society for Testing and Materials (ASTM) are followed. Prospective studies also provide valuable information (Faraj and Webb 1997; Lonstein et al. 1999; Prud'homme et al. 2014). Finite Element Analysis (FEA) is a very powerful investigative tool, used complementary to experimental studies (Hsu et al. 2005; Zhang et al. 2006; Chao et al. 2008; Amaritsakul et al. 2014; Demir and Basgül 2015; Rosa et al. 2016). Parameters describing

both the screw design and the bone can be varied, thereby allowing the study of the underlying biomechanical mechanisms determining the screw performance. However, model validation is essential. Generally, this is based on data obtained from pullout or bending experiments on pedicle screws inserted in bone-mimicking foam (Hsu et al. 2005; Chao et al. 2008; Amaritsakul et al. 2014; Rosa et al. 2016). A similar observation is made when reviewing studies on bone screws (Shirazi-Adl et al. 2001; Hou et al. 2004; Chao et al. 2007). Such models allow comparative analyses and a qualitative evaluation of the effect of bone mineral density (BMD). However, this procedure does not take into account the variability in mechanical properties and macro- and micro-architecture of the human vertebrae. To the authors' knowledge, none of the existing Finite Element (FE) models have been validated with cadaveric vertebrae.

The purpose of the present study is therefore to develop a patient-specific FE model of a standard cylindrical pedicle screw inserted in the lumbar vertebra, of which the numerical behavior is evaluated against the *in vitro* recorded behavior, to predict the intraoperative pullout strength. µCT imaging will enable the estimation of the material properties, as well as the precise modeling and meshing of the bone.

2. Materials and methods

2.1. Experimental study

The pullout resistance of 30 cadaveric vertebrae (T12, L4 and L5) was assessed experimentally with a commercially available Ti-6Al-4V cylindrical pedicle screw with a trapezoidal thread shape (Fradis Medical, Salouël, France). The geometrical parameters of the screw as provided by the manufacturer are given in Table 1. The cadaveric samples were fresh frozen immediately after harvesting and gently thawed at room temperature before testing. BMD was assessed with a DXA device (QDR 4500/A, Hologic, Waltham, MA, USA). The T-score for seven of the ten donors was inferior to –2.5, indicating osteoporosis. One donor was found osteopenic, with a T-score between –2.5 and –1. The bone mineral density of the two other donors was considered normal (World Health Organisation

1994). The mean age was 81.8 years (std. ± 7.8 years) and the distribution female/male was 6 to 4.

For the measurement of the pullout force, a pedicle screw was inserted unilaterally in each of the 30 vertebrae. The screw dimensions were the same for all tested vertebrae, thus correcting for the effect of changing screw dimensions on the pullout strength. The location of insertion, i.e. the left or right pedicle, was randomized. The screw insertion point for the lumbar vertebrae was the *processus mammillaris* (Ouellet and Arlet 2004). For the thoracic vertebrae, the insertion point was defined by the crossing of the base of the superior facet joint and the *processus transversus* (Ebraheim et al. 1997). Guiding holes were made in the pedicle with a surgical curved awl and were checked for breaches before screw insertion. The screws were inserted without tapping. The screw insertion was performed by an experienced orthopedic surgeon. A µCT image was taken before and after screw insertion with a µCT 100 device (SCANCO Medical AG, Brüttisellen, Switzerland). The resolution was set to 88 µm (Hulme et al. 2007). The vertebra was immobilized in polymethylmethacrylate (PMMA) (Technovit®, Buehler, Düsseldorf, Germany), with the pedicle screw oriented vertically upwards and the vertebral body completely submerged (see Figure 1(a)). A biplanar X-ray image was taken with an EOS system (EOS imaging SA., Paris, France) to evaluate the positioning of the screw inside the pedicle (see Figure 1(b)).

A uniaxial traction test was performed on the screw on an INSTRON 5566 test bench (Instron Industrial Products, Grove City, PA, USA). A constant rate of displacement of 5 mm/min was applied in the direction of the screw axis. Axial forces were measured until a displacement of ±5 mm was reached. This displacement was high enough to yield complete screw loosening.

The pullout strength was defined as the maximum of the force-displacement curve. The slope of the linear part of the force-displacement curve was chosen as a measure for the pullout stiffness.

2.2. Finite element modeling

The finite element analysis was performed using ANSYS 15.0 (ANSYS Inc., Cannonsburg, PA, USA). The FE model consists of two parts: the screw and the bone in contact with it, i.e. the pedicle and part of the vertebral body.

2.2.1. Screw model

The screw geometry was parameterized and modeled with the ANSYS Parametric Design Language (APDL). The defining parameters are pitch, inner and outer diameter, thread width, thread depth, thread angles and number of threads. The screw geometry was obtained as a

Table 1. Geometrical dimensions of the pedicle screw used in the experimental study.

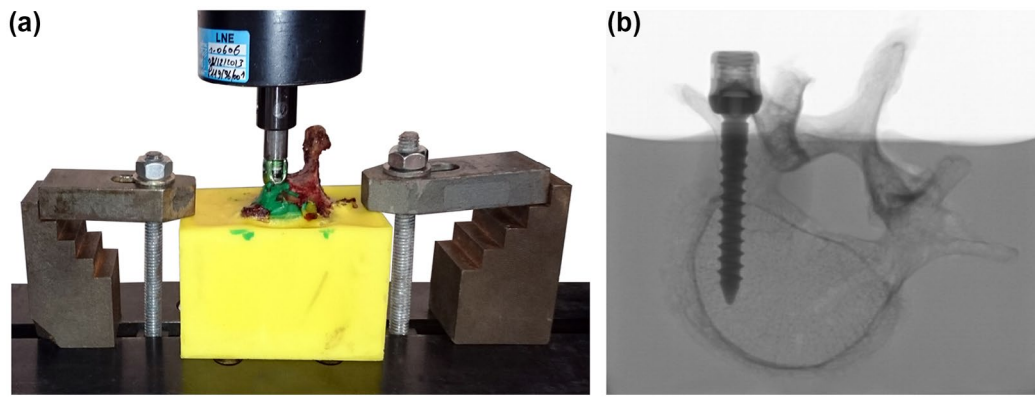|	
Outer diameter	6.1 mm
Core diameter	4.3 mm
Pitch	2.8 mm
Proximal thread angle	15°
Distal thread angle	30°
Thread width	0.2 mm

Figure 1. (a) The experimental set-up. The figure depicts the cadaveric vertebra, immobilized in PMMA, mounted on the test bench. (b) An X-ray image in the axial plane showing the positioning of the screw in the pedicle.

helical assembly of hexahedral elements. The eight-node SOLID45 element with three degrees of freedom (DOF) per node was selected. As such, the geometrical characteristics of the screw threads could be replicated and an appropriate connection between the threads and the screw core at the node level could be obtained. However, as a consequence of this helical architecture, it was not possible to completely fill the screw volume (see also Figure 2). Preliminary simulations have shown that the effect of the cylindrical hole on the model behavior is however insignificant. Figure 2 gives a visual representation of the model. An elastic modulus of 110 GPa and a Poisson's ratio of 0.3 were chosen, corresponding to the mechanical properties of Ti-6Al-4V (Combres 2010; Mulier 2012). The mechanical behavior was considered isotropic and linear elastic.

2.2.2. Morphorealistic bone model
The bone model incorporates the information regarding pedicle morphology and material properties from the μCT
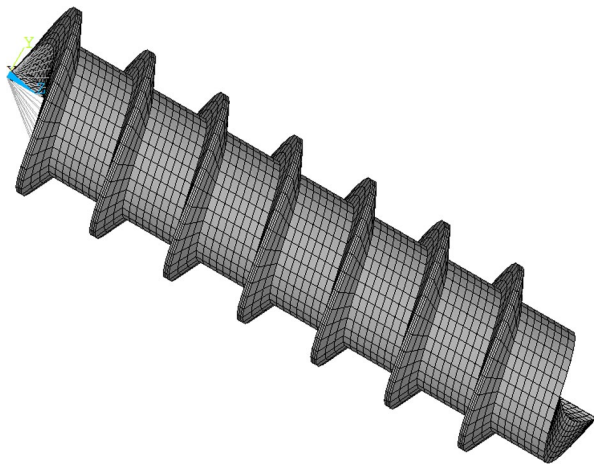

Figure 2. The screw model. The screw was modeled as a helical assembly of hexahedral elements.

images. Mimics 15.0 (Materialise, Leuven, Belgium) was used to segment the μCT images and to create a 3D-model of the bone in contact with the screw. The image taken after screw insertion was used to indicate the region of interest (ROI) on the image taken before screw insertion. Since the image showing the screw suffers from artefacts, it was not used further in the modeling procedure. A triangularsurface mesh was exported to Matlab R2011b (The Mathworks Inc., Natick, MA, USA) to create a volume mesh. A generic cylindrical hexahedral volume mesh was deformed to match the contours of the ROI, resulting from the μCT image segmentation (see Figure 3). The bone volume was meshed with the same eight-node hexahedral elements as those used for the screw model. Four-node SHELL181 elements were used to mesh the outer cortical layer. Because the μCT images do not allow an unambiguous delineation of the cortical bone, the shell elements were appointed a constant thickness of 0.35 mm. This value was based on the measurement of the lateral wall thickness of one sample with low and one with high BMD and on literature data (Ritzel et al. 1997).

The ROI was divided into two subdomains, namely the vertebral body and the pedicle. In both domains, the porosity of the cancellous bone was calculated voxel-based from the μCT scans and used to estimate the Young's modulus and the yield strength, using an adapted form of the power-law described by Goulet et al. (1994) (Goulet et al. 1994). The result is a homogenous mesh with the same mechanical properties for each finite element. The mechanical properties for the cortical bone were derived from Bartel et al. (2006) (Bartel et al. 2006). A linear elastic/perfectly plastic isotropic constitutive equation was assumed for both the cortical and the cancellous bone (Zhang et al. 2004, 2006; Chatzistergos et al. 2010), since the bony elements do not contribute anymore to the system's stiffness when the plastic limit has been reached.
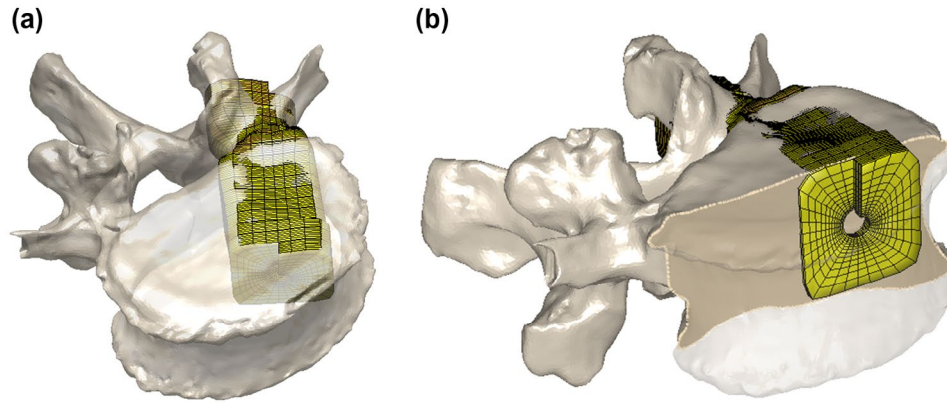
Figure 3. (a) The morphorealistic model of the pedicle in relation to the complete vertebra. The model represents the pedicle and part of the corpus. (b) An antero-lateral section view of the vertebra showing the distal surface of the model. Note the local mesh refinement close to the screw.

At the trailing surface of the screw threads, the screw/bone interface was modeled with surface-to-surface contact elements in an initially bonded contact configuration (Zhang et al. 2004, 2006; Chatzistergos et al. 2010). Frictionless contact was considered, since the pullout force was perfectly aligned with the screw axis and failure occurs at the thread tips (Chatzistergos et al. 2010). The surface of the screw was meshed with CONTA173 elements. The complementary surface of the bone was meshed with TARGE170 elements. The screw/bone interface at the leading surface of the screw threads was modeled differently. Contact elements were not used in order to allow interface debonding (see also Figure 8). Local mesh refinement was performed around the screw up to around 5% of the maximum element size, which is determined by the pedicle diameter. This level of refinement was obtained through a mesh convergence analysis.

The external surface of the model corresponding to the vertebral body was fully constrained in all DOF. The pullout experiment was simulated as a quasi-static process, during which a displacement was applied incrementally at the screw tip in the direction of the screw axis. To avoid too high deformations at the element level, the maximum applied displacement was limited to 0.5 mm. As the analysis of experimental data revealed a high positive correlation between the force at 0.5 mm displacement and the pullout strength (Pearson $\rho = 0.996$, $p = 2.89 \ 10^{-5}$), the numerical strength was defined as the numerical force obtained at an applied displacement of 0.5 mm.

2.3. Preliminary validation

As a first step, the L4 vertebral level was considered. Six cadaveric samples were selected, for each of which an FE model was created. The numerical results were compared with the corresponding *in vitro* test results. A one-to-one comparison between the experimental and numerical pullout stiffness and force at 0.5 mm displacement was performed.

2.4. Statistical analyses

The experimental pullout strength and stiffness were correlated with the BMD. Also, the correlation between the experimental pullout strength and stiffness was evaluated.

The normality of the data was verified with a Shapiro-Wilk test. In case the data could be assumed normally distributed, the correlation analysis was performed with the Pearson coefficient. If not, its non-parametric alternative, i.e. the Spearman coefficient, was used instead. The one-to-one comparison was performed with the non-parametric Wilcoxon Signed Rank test. Contrary to the parametric paired t-test, the Wilcoxon Signed Rank is not based on the mean differences, such that large negative and positive differences cannot cancel out each other. The significance level was fixed at 0.05.

3. Results

3.1. Experimental study

Force-displacement curves were obtained for each of the 30 cadaveric vertebrae (see Figure 4). A moderate positive correlation between BMD and pullout strength was noted (Spearman $\rho = 0.59$, $p = 6.81 \ 10^{-4}$). A high positive correlation was found between pullout strength and stiffness (Spearman $\rho = 0.84$, $p = 8.00 \ 10^{-7}$), as well as between pullout strength and the force at 0.5 mm displacement (Pearson $\rho = 0.996$, $p = 2.89 \ 10^{-5}$).

The porosity measurements in the vertebral body and the pedicle revealed no significant difference, the result of a paired t-test ($p = 0.66$).
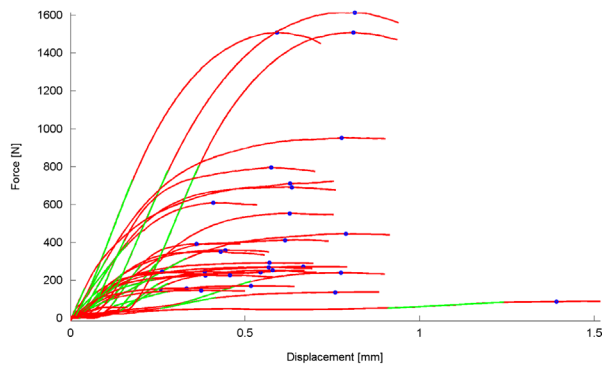
Figure 4. The force-displacement data for each of the 30 cadaveric vertebrae. The green lines indicate the linear part of the curve and represent the least squares regression line for a subset of the data points. The blue dots indicate the force values used as a measure for the pullout strength.

3.2. Numerical study

Figure 5 depicts the numerical force-displacement curves for the six modeled cadaveric vertebrae, in relation to the corresponding experimental curves. Figure 6(a) and (b) compare the experimental with numerical pullout force and stiffness data, respectively. It was found that the numerical strength correlates well with the experimental pullout strength (Pearson $\rho = 0.87$, $p = 0.023$). A stronger positive correlation (Pearson $\rho = 0.90$, $p = 0.016$) was noticed between the numerical and experimental force at 0.5 mm displacement, with differences ranging between 99 N and 571 N. A significant positive correlation was also found between the numerical and experimental pullout stiffness (Pearson $\rho = 0.96$, $p = 0.0028$).

4. Discussion

The aim of this study was the development and validation of a subject-specific FE model of a cylindrical pedicle screw inserted in the lumbar vertebra. Literature describes few FE models investigating the mechanical behavior of pedicle screws in relation to the morphorealistic vertebra
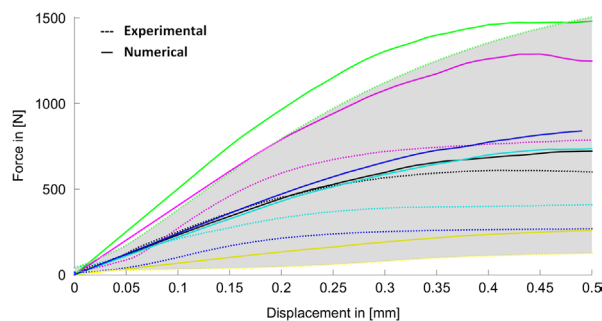

Figure 5. Comparison between the experimental and numerical force-displacement curves obtained for six of the tested cadaveric vertebrae.

(Chen et al. 2003; Wang et al. 2014), while such models might provide a better understanding of the still often reported issue of screw loosening (Prud'homme et al. 2014). Naturally, the model should be validated with experimental data to prove its clinical relevance. As a first attempt, the biofidelity is often established based on experiments performed on screws inserted in bone-mimicking foam (Dammak et al. 1997; Shirazi-Adl et al. 2001; Hou et al. 2004; Hsu et al. 2005; Chao et al. 2008; Amaritsakul et al. 2014). However, the inter-subject variability in bone morphology and material properties is not considered. To the best of the authors' knowledge, this is the first study to present a subject-specific model with personalized material properties, incorporating the real morphology of the ROI and for which a preliminary validation against *in vitro* experiments has been performed.

The experimental study was conducted to allow the exact replication of the set-up in the FE model. Hence, the boundary conditions as well as the orientation and direction of the applied force were carefully controlled. Table 2 presents the measured pullout force and stiffness in relation to the results described in literature. Although a direct comparison is not easy because of the variety of experimental set-ups, the observed inter-subject variability is consistent with the literature and can be ascribed to the variability in bone quality: the youngest subject produced significantly higher pullout force and stiffness values than the rest of the population (see also Figure 4).

It should be noted that the experimental analysis performed in this study replicated the conditions of a worst-case scenario: the pullout force was aligned perfectly parallel to the screw axis. This explains the lower values reported in this study. However, the conditions of this scenario were perfectly controllable, allowing a detailed one-to-one comparison with the numerical results.

The FE model was conceived to meet three main requirements. Firstly, the model should accurately replicate the real geometry of the vertebra, which was obtained through μCT-imaging. An appropriate mesh, with optimal ratio between precision and calculation time, was obtained through a convergence analysis. Figures 3 and 7 show that the model accurately replicates the morphology of the ROI, i.e. the contours of the model match those of the real pedicle.

Another important model feature is the material behavior. In this study, the porosity was chosen as an estimator for the Young's modulus and the strength of the cancellous bone. However, few validated relations are available in literature (Goulet et al. 1994). Moreover, literature data was used to determine the mechanical properties of the cortical bone (Bartel et al. 2006). This might be an explanation for the large differences between the experimental and numerical results for two of the six samples. An
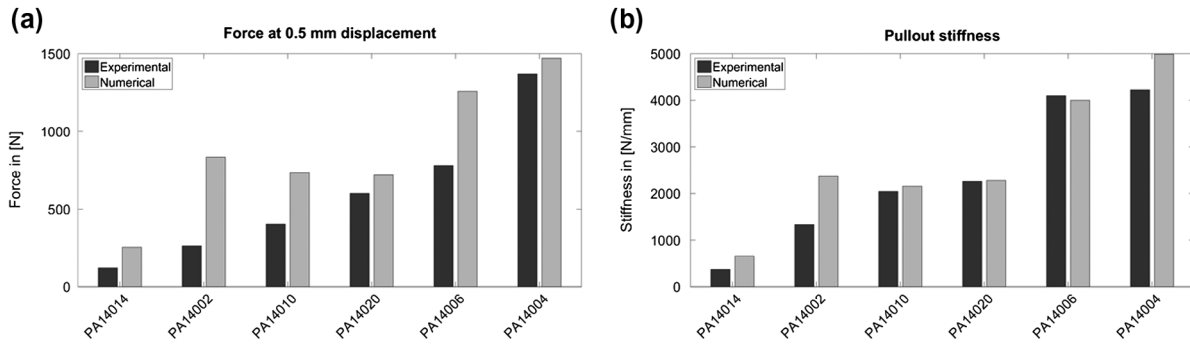
Figure 6. (a) The experimental vs. numerical force at 0.5 mm displacement. The samples are sorted by experimental force. The model seems to be able to correctly differentiate the samples, since the smallest predicted pullout force corresponds to the smallest experimental force. (b) The experimental vs. numerical pullout stiffness. The samples are sorted by experimental stiffness. The model seems to be able to correctly differentiate the samples, since the smallest predicted pullout stiffness corresponds to the smallest experimental pullout stiffness.

Table 2. Comparison of the experimental results regarding pullout force and stiffness obtained in this study with the relevant literature.

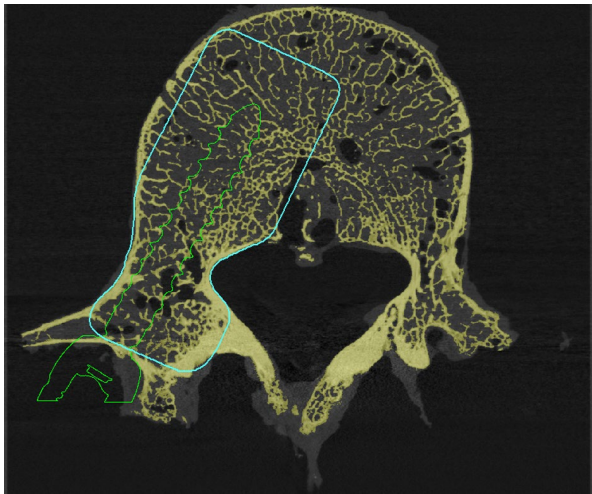| Author (year)		#Donors	#Samples	Age [years]	Gender	Force [N]	Stiffness [N/mm]
	Group 1	1	3	61 (±0)	1 M	1543 (±62)	4428 (±261)
Current study	Group 2	9	27	84 (±3)	3 M/6F	356 (±223)	2065 (±1303)
Liljenqvist et al. (2001)		9	72	74 (/)	2 M/7F	808 (±207)	Estimated to 700
Chou et al. (2014)		6	12	64 (±17)	5 M/1F	1075 (±199)	/
Kang et al. (2014)		11	31	/	/	742 (± 320)	/
Ordway et al. (2005)		6	36	70–89	6F	703 (±459)	/

Figure 7. The contours of the morphorealistic model in relation to the μCT image of the corresponding vertebra.

improvement might be to use the Hounsfield Unit (HU) instead of the porosity to estimate the material properties (Rho et al. 1995).

As third and last model requirement, the model should be able to reproduce the experimental load-displacement behavior (see Figure 4). Pullout strength and stiffness were considered for model validation. The preliminary model evaluation based on six specimens, yielded promising results. Regardless of the model limitations, the pullout stiffness predictions show a high positive correlation with the linear part of the experimental force-displacement curves. The experimental force at 0.5 mm displacement also correlates well with its numerical equivalent. Although the model does not exactly reproduce the experimental stiffness and strength, it does differentiate between samples with varying bone quality and geometry and respects the experimental corridor (see also Figure 5). While a weak positive correlation was found between pullout strength and BMD ($\rho = 0.59$), a stronger positive correlation was obtained with the numerical model, which also considers bone geometry ($\rho = 0.87$). This shows that the difference in morphology is an important explanatory factor for the variance in mechanical behavior of the different samples. The rather low variance in porosity and the lack of difference between porosity in the vertebral body and the pedicle, merely confirm this finding.

The Von Mises stress criterion was used to define failure at the element level, which allowed rendering a nonlinear behavior. Since this criterion is based on an equivalent stress, the failure limit might be overestimated. The experimental and numerical strength were slightly less correlated than the experimental and numerical force at 0.5 mm displacement (0.87 vs. 0.90). A more refined failure criterion thus seems necessary.

Although several studies used frictionless screw/bone contact conditions (Hou et al. 2004; Hsu et al. 2005; Chao
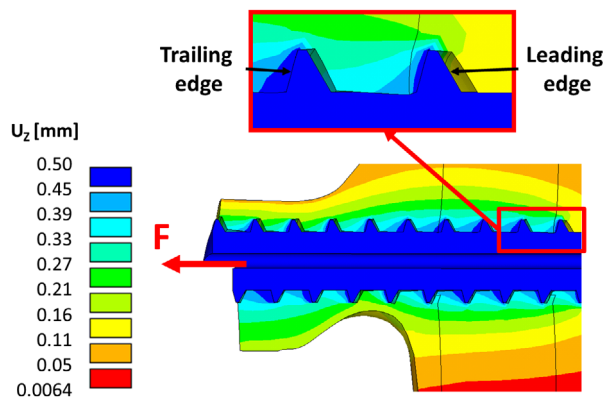
Figure 8. A contour plot visualizing the displacement in the pullout direction. Note that the screw loses contact with the bone at its leading edge.

et al. 2008), Dammak et al. (1997) (Dammak et al. 1997) and Shirazi-Adl et al. (2001) (Shirazi-Adl et al. 2001) found that this is not a realistic description of the screw/bone interface, at least under bending loads. However, these authors did not explicitly model the screw threads. MacLeod et al. (2012) (MacLeod et al. 2012) illustrated that when doing so, the contact condition has a less significant effect on the load-displacement behavior. Moreover, since the pullout force was directed in the axis of the screw, the main loading at the screw/bone interface was compression. Also, Chatzistergos et al. (2010) (Chatzistergos et al. 2010) found that failure occurs at the thread tip, which was confirmed in this study (see Figure 8).

Another shortcoming of the model is the representation of the cortical outer layer of the pedicle by a thin layer of constant thickness. As can be observed on μCT images, the layer thickness is not constant. Hence, further improvement exists in using shell elements of which the thickness changes as a function of location.

A last limitation of the model is that bone compaction due to screw insertion, altering the mechanical behavior of the bone in the screw vicinity and possibly adding to the pullout strength, was not considered. Future work could consider this aspect, but even with this simplification, the results are already quite consistent with the experimental behavior.

The screw model presented here is parameterized, enabling the adjustment of specific design parameters such as inner diameter, outer diameter and pitch. It is thus possible to replicate the morphology of a broad range of commercially available screws.

In conclusion, it can be stated that the model, regardless of its limitations, provides promising results. The model offers a qualitative estimation for the pullout stiffness and strength. Even though improvements are to be made, this work is an important step to obtain a fully validated subject-specific model. This is the first study presenting

a model with subject-specific geometry and material properties and of which the predictions are compared one-to-one with *in vitro* measurements. After a more in-depth validation, this model might be used to propose screw design adjustments.

Acknowledgements

Disclosure statement

No potential conflict of interest was reported by the authors.

Funding

References

Amaritsakul Y, Chao C-K, Lin J. 2014. Biomechanical evaluation of bending strength of spinal pedicle screws, including cylindrical, conical, dual core and double dual core designs using numerical simulations and mechanical tests. Med Eng Phys [Internet]. 36:1218–1223. http://www.ncbi.nlm.nih.gov/pubmed/25060212.

Arslan AK, Demir T, Örmeci MF, Camuscu N, Türeyen K. 2013. Postfusion pullout strength comparison of a novel pedicle screw with classical pedicle screws on synthetic foams. Proc Inst Mech Eng Part H J Eng Med [Internet]. 227:114–119. http://pih.sagepub.com/lookup/doi/10.1177/0954411912463323.

Aycan MF, Tolunay T, Demir T, Yaman ME, Usta Y. 2017. Pullout performance comparison of novel expandable pedicle screw with expandable poly-ether-ether-ketone shells and cement-augmented pedicle screws. Proc Inst Mech Eng Part H J Eng Med [Internet]. 231:169–175. http://journals.sagepub.com/doi/10.1177/0954411916687792.

Bartel DL, Davy DT, Keaveny TM. 2006. Orthopaedic biomechanics, mechanics and design in musculoskeletal systems. London: Pearson Education Inc.

Cetin E, Özkaya M, Güler ÜO, Acaroglu E, Demir T. 2015. Evaluation of the effect of fixation angle between polyaxial pedicle screw head and rod on the failure of screw-rod connection. Appl Bionics Biomech. 2015:9 pages.

Chamoli U, Diwan AD, Tsafnat N. 2014. Pedicle screw-based posterior dynamic stabilizers for degenerative spine: In vitro biomechanical testing and clinical outcomes. J Biomed Mater Res A [Internet]. 102:3324–3340. http://www.ncbi.nlm.nih.gov/pubmed/24382799.

Chao C-K, Hsu C-C, Wang J-L, Lin J. 2007. Increasing bending strength of tibial locking screws: mechanical tests and finite element analyses. Clin Biomech (Bristol, Avon) [Internet]. 22:59–66. http://www.ncbi.nlm.nih.gov/pubmed/16959388

Chao C-K, Hsu C-C, Wang J-L, Lin J. 2008. Increasing bending strength and pullout strength in conical pedicle screws: biomechanical tests and finite element analyses. J Spinal Disord Tech. 21:130–138.

Chatzistergos PE, Magnissalis EA, Kourkoulis SK. 2010. A parametric study of cylindrical pedicle screw design implications on the pullout performance using an experimentally validated finite-element model. Med Eng Phys [Internet]. 32:145–154. http://www.ncbi.nlm.nih.gov/pubmed/19945333.

Chen SI, Lin RM, Chang CH. 2003. Biomechanical investigation of pedicle screw–vertebrae complex: a finite element approach using bonded and contact interface conditions. Med Eng Phys [Internet]. 25:275–282. http://linkinghub.elsevier.com/retrieve/pii/S1350453302002199.

Chou WK, Chien A, Wang JL. 2014. Pullout strength of thoracic pedicle screws improved with cortical bone ratio: a cadaveric study. J Orthop Sci. 19(6):900–906.

Combres Y. 2010. Propriétés du titane et de ses alliages [Properties of titanium and its alloys] [Internet]. [accessed 2015 Oct 16]. http://www.techniques-ingenieur.fr/base-documentaire/biomedical-pharma-th15/biomateriaux-et-biomecanique-42606210/proprietes-du-titane-et-de-ses-alliages-m4780/.

Dammak M, Shirazi-Adl A, Zukor DJ. 1997. Analysis of cementless implants using interface nonlinear friction - Experimental and finite element studies. J Biomech. 30:121–129.

Demir T, Basgül C. 2015. The pullout performance of pedicle screws. In: Altenbach H, da Silva L F M, Öchsner A, editors. Springer Briefs in Applied Sciences and Technology - Computational Mechanics. Springer International Publishing.

Demir T, Camuşcu N, Türeyen K. 2012. Design and biomechanical testing of pedicle screw for osteoporotic incidents. Proc Inst Mech Eng Part H J Eng Med [Internet]. 226:256–262. http://pih.sagepub.com/content/226/3/256.short\nhttp://pih.sagepub.com/lookup/doi/10.1177/0954411911434680.

Ebraheim NA, Xu R, Ahmad M, Yeasting RA. 1997. Projection of the thoracic pedicle and its morphometric analysis. Spine (Phila Pa 1976). 22:233–238.

Faraj AA, Webb JK. 1997. Early complications of spinal pedicle screw. Eur Spine J. 6:324–326.

Goulet RW, Goldstein SA, Ciarelli MJ, Kuhn JL, Brown MB, Feldkamp LA. 1994. The relationship between the structural and orthogonal compressive properties of trabecular bone. J Biomech. 27:375–389.

Hadjipavlou A, Enker P, Dupuis P, Katzman S, Silver J. 1996. The causes of failure in transpedicular spinal instrumentation and fusion. Int Orthop. 20:35–42.

Hou S-M, Hsu C-C, Wang J-L, Chao C-K, Lin J. 2004. Mechanical tests and finite element models for bone holding power of tibial locking screws. Clin Biomech (Bristol, Avon) [Internet]. 19:738–745. http://www.ncbi.nlm.nih.gov/pubmed/15288461

Hsu CC, Chao CK, Wang JL, Hou SM, Tsai YT, Lin J. 2005. Increase of pullout strength of spinal pedicle screws with conical core: Biomechanical tests and finite element analyses. J Orthop Res. 23:788–794.

Hulme PA, Boyd SK, Ferguson SJ. 2007. Regional variation in vertebral bone morphology and its contribution to vertebral fracture strength. Bone [Internet]. 41:946–957. http://www.ncbi.nlm.nih.gov/pubmed/17913613.

Kang DG, Lehman RA, Wagner SC, Bevevino AJ, Bernstock JD, Gaume RE, Dmitriev AE. 2014. Pedicle screw reinsertion using previous pilot hole and trajectory does not reduce fixation strength. Spine. 39(20):1640–1647.

Kim Y-Y, Choi W-S, Rhyu K-W. 2012. Assessment of pedicle screw pullout strength based on various screw designs and bone densities – an ex-vivo biomechanical study. Spine J [Internet]. 12:164–168. http://www.ncbi.nlm.nih.gov/pubmed/22336467.

Liljenqvist U, Hackenberg L, Link T, Halm H. 2001. Pullout strength of pedicle screws versus pedicle and laminar hooks in the thoracic spine. Acta Orthop Belg. 67:157–163.

Lonstein JE, Denis F, Perra JH, Pinto MR, Smith MD, Winter RB. 1999. Complications associated with pedicle screws. J Bone Jt Surg. 81:1519–1528.

MacLeod AR, Pankaj P, Simpson AHRW. 2012. Does screw-bone interface modelling matter in finite element analyses? J Biomech [Internet]. 45:1712–1716. http://www.ncbi.nlm.nih.gov/pubmed/22537570.

MedTech Insight. 2006. European markets for spinal fusion products [Internet]. [accessed 2015 Oct 16]. http://www.medtechinsight.com/ReportA306.html.

Mulier M. 2012. Functional anatomy of the human locomotor system: course notes. Leuven: Katholieke Universiteit Leuven.

Okuyama K, Abe E, Suzuki T, Tamura Y, Chiba M, Sato K. 2001. Influence of bone mineral density on pedicle screw fixation: a study of pedicle screw fixation augmenting posterior lumbar interbody fusion in elderly patients. Spine J. 1:402–407.

Ordway N, Wilson T, Buerkle T, Yan HA. 2005. Lumbar pedicle screw fixation in osteoporotic bone: a technique utilizing PMMA and a fenestrated screw. In: Transactions of the 51st Annual Meeting of the Orthopaedic Research Society; February 20–23; Washington, DC.

Ouellet JA, Arlet V. 2004. Surgical anatomy of the pelvis, sacrum, and lumbar spine relevant to spinal surgery. Semin Spine Surg [Internet]. 16:91–100. http://linkinghub.elsevier.com/retrieve/pii/S1040738304000346.

Prud'homme M, Barrios C, Rouch P, Charles YP, Steib J-P, Skalli W. 2014. Clinical outcomes and complications after pedicle-anchored dynamic or hybrid lumbar spine stabilization: a systematic literature review. J Spinal Disord Tech [Internet]. http://www.scopus.com/inward/record.url?eid=2-s2.0-84905318535&partnerID=tZOtx3y1.

Rajaee SS, Bae HW, Kanim LE, Delamarter RB. 2012. Spinal fusion in the United States: analysis of trends from 1998 to 2008. Spine (Phila Pa 1976) [Internet]. 37:67–76. http://linkinghub.elsevier.com/retrieve/pii/S1529943012001167.

Rho JY, Hobatho MC, Ashman RB. 1995. Relations of mechanical properties to density and CT numbers in human bone. Med Eng Phys. 17:347–355.

Ritzel H, Amling M, Pösl M, Hahn M, Delling G. 1997. The thickness of human vertebral cortical bone and its changes in aging and osteoporosis: a histomorphometric analysis of the complete spinal column from thirty-seven autopsy specimens. J Bone Miner Res. 12:89–95.

Rosa G, Clienti C, Mineo R, Audenino A. 2016. Experimental analysis of pedicle screws. Procedia Struct Integr [Internet].

2:1244–1251. http://linkinghub.elsevier.com/retrieve/pii/S2452321616301676.

Shirazi-Adl A, Dammak M, Zukor DJ. 1994. Fixation pull-out response measurement of bone screws and porous-surfaced posts. J Biomech. 27:1249–1258.

Shirazi-Adl A, Patenaude O, Dammak M, Zukor D. 2001. Experimental and finite element comparison of various fixation designs in combined loads. J Biomech Eng. 123:391–395.

Wang W, Baran GR, Garg H, Betz RR, Moumene M, Cahill PJ. 2014. The benefits of cement augmentation of pedicle screw fixation are increased in osteoporotic bone: a finite element analysis. Spine Deform [Internet]. 2:248–259. http://linkinghub.elsevier.com/retrieve/pii/S2212134X14000318.

World Health Organisation. 1994. Assessment of fracture risk and its implication to screening for postmenopausal osteoporosis. Geneva. Technical Report Number 843.

Yaman O, Demir T, Arslan AK, Iyidiker MA, Tolunay T, Camuscu N, Ulutas M. 2015. The comparison of pullout strengths of various pedicle screw designs on synthetic foams and ovine vertebrae. Turk Neurosurg. 25:532–538.

Zhang QH, Tan SH, Chou SM. 2004. Investigation of fixation screw pull-out strength on human spine. J Biomech [Internet]. 37:479–485. http://www.ncbi.nlm.nih.gov/pubmed/14996559.

Zhang QH, Tan SH, Chou SM. 2006. Effects of bone materials on the screw pull-out strength in human spine. Med Eng Phys [Internet]. 28:795–801. http://www.ncbi.nlm.nih.gov/pubmed/16414303.